

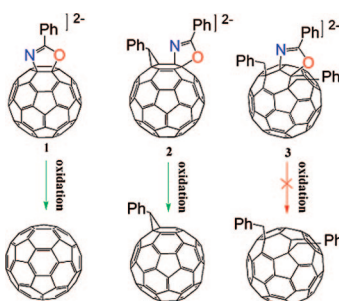
Why [6,6]- and 1,2-Benzal-3-*N*-4-*O*-Cyclic Phenylimidate C₆₀ Undergo Electrochemically Induced Retro-Addition Reactions while 1,4-Dibenzyl-2,3-Cyclic Phenylimidate C₆₀ Does Not? C–H···X (X = N, O) Intramolecular Interactions in Organofullerenes

Fang-Fang Li, Xiang Gao,* and Min Zheng

State Key Laboratory of Electroanalytical Chemistry, Changchun Institute of Applied Chemistry, Graduate School of Chinese Academy of Sciences, Chinese Academy of Sciences, 5625 Renmin Street, Changchun, Jilin 130022, China

xgao@ciac.jl.cn

Received August 07, 2008



The electrochemical properties of a series of structurally related fullerooxazoles, [6,6] cyclic phenylimidate C₆₀ (**1**), 1,2-benzal-3-*N*-4-*O*-cyclic phenylimidate C₆₀ (**2**), and 1,4-dibenzyl-2,3-cyclic phenylimidate C₆₀ (**3**), are described, and the spectroscopic characterizations of their anionic species are reported. The results show that compounds **1** and **2** undergo retro-cycloaddition reactions that lead to the formation of C₆₀ and C₆₁HPh, respectively, upon two-electron-transfer reduction. However, compound **3** demonstrates much more electrochemical stability as no retro-cycloaddition reaction occurs under similar conditions. Natural bond orbital (NBO) calculations on charge distribution show there is no significant difference among the dianions of **1**, **2**, and **3**, indicating that the electrochemical stability of **3** is unlikely to be caused by the charge distribution difference of the dianions of three compounds. Examination on the crystal structure of compound **3** reveals close contacts of the C–H group with the heteroatoms (N and O) of cyclic phenylimidate, suggesting the existence of C–H···X (X = N, O) intramolecular hydrogen bonding among the addends, which is further confirmed by NBO analysis. The results thus suggest that intramolecular hydrogen bonding is responsible for the electrochemical stability of **3**.

Introduction

Functionalization of fullerenes has been attracting great interest¹ as the potential of fullerene derivatives has been demonstrated in various areas, for example, photovoltaic materials² and medicinal chemistry.³ However, many kinds of orga-

nofullerenes are not stable and are subjected to retro-addition reactions. It has been shown that malonate and spiromethano addends on C₆₀ can be removed under reductive conditions,⁴ while pyrrolidino groups are cleaved under oxidative elec-

(1) (a) Taylor, R.; Walton, D. R. M. *Nature* **1993**, *363*, 685–693. (b) Diederich, F.; Thilgen, C. *Science* **1996**, *271*, 317–323. (c) Prato, M.; Maggini, M. *Acc. Chem. Res.* **1998**, *31*, 519–526. (d) Hirsch, A.; Brettreich, M. *Fullerenes: Chemistry and Reactions*; Wiley-VCH: Weinheim, Germany, 2005. (e) Martín, N. *Chem. Commun.* **2006**, 2093–2104.

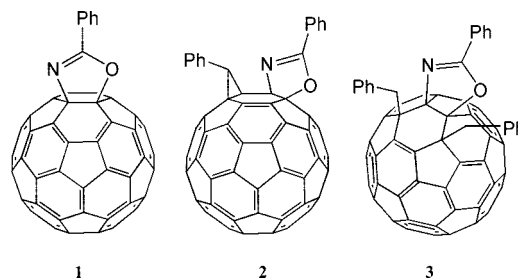
(2) (a) Kim, J. Y.; Lee, K.; Coates, N. E.; Moses, D.; Nguyen, T.-Q.; Dante, M.; Heeger, A. J. *Science* **2007**, *317*, 222–225. (b) Yang, X.; Lu, G.; Li, L.; Zhou, E. *Small* **2007**, *3*, 611–615. (c) Kamat, P. V. *J. Phys. Chem. C* **2007**, *111*, 2834–2860.

(3) (a) Tagmatarchis, N.; Shinohara, H. *Mini-Rev. Med. Chem.* **2001**, *1*, 339–348. (b) Da Ros, T.; Spalluto, G.; Prato, M. *Croat. Chem. Acta* **2001**, *74*, 743–755. (c) Nakamura, E.; Isobe, H. *Acc. Chem. Res.* **2003**, *36*, 807–815.

tolysis and thermal conditions,⁵ while heterocyclic pyrazolino and isoxazolino rings are removed under thermal conditions in the presence of dipolarophiles.⁶ Although such retro-addition reactions have shown promising application in the protection/deprotection strategy for the purification and functionalization of fullerenes,^{4b–d,5a} the reactions may cause problems for the applications of organofullerenes due to the instability of the compounds. It is important, therefore, to investigate any factors that affect the stability of organofullerenes.

Hydrogen bonding of C–H···X (X = N, O)⁷ has been recognized since the early 1980s after a long-time controversy,⁸ where the C–H group acts as a proton donor to acceptors. Despite the C–H···X hydrogen bond's relative weakness, the bond has played important roles in supramolecular chemistry,^{7c,d} structural arrangement and function of biological molecules,⁹ crystal packing and engineering,^{7c} and stabilization of molecular complexes.¹⁰ The formation of a C–H···X hydrogen bond can be evaluated effectively using natural bond orbital (NBO) analysis,¹¹ where information on the population of lone pairs and antibonding orbital ($\sigma^*(\text{C}-\text{H})$) involved in the hydrogen bond, stabilization energy ($E^{(2)}$), as well as the changes to the charge densities of proton donors and acceptors can be obtained. Reports of C–H···X interactions in both inter- and intramo-

CHART 1



lecular hydrogen bonds are extensive.^{7–10} However, work on C–H···X bonding in the field of fullerene derivatives is very limited. The few available examples are all related to the intermolecular C–H···O hydrogen bonds.¹² No report on intramolecular C–H···X hydrogen bonding which might improve the stability of organofullerenes has appeared to date.

Recently, a series of fulleroroxazoles,¹³ [6,6] cyclic phenylimidate C₆₀ (**1**),^{13a} 1,2-benzal-3-N-4-O-cyclic phenylimidate C₆₀ (**2**),^{13b} and 1,4-dibenzyl-2,3-cyclic phenylimidate C₆₀ (**3**)^{13a} (Chart 1) have been synthesized. Electrochemical and spectroelectrochemical studies show that compounds **1** and **2** undergo retro-cycloaddition reactions, and the cyclic phenylimidate group is removed under two-electron-transfer reductive electrolysis. However, no retro-cycloaddition reaction occurs for compound **3** under the same conditions, indicating that the heterocyclic phenylimidate in compound **3** is stabilized somehow. Herein, different behavior of **1**, **2**, and **3** under reductive electrolysis is reported, and the mechanism responsible for the difference is investigated.

Results and Discussion

Fulleroroxazoles **1**, **2**, and **3** were synthesized and purified as previously described.^{13a,b} The cyclic voltammograms of **1–3** in DMF containing 0.1 M tetrabutylammonium perchlorate (TBAP) are shown in Figure 1. The compounds all undergo a reversible one-electron reduction–oxidation (redox) process for

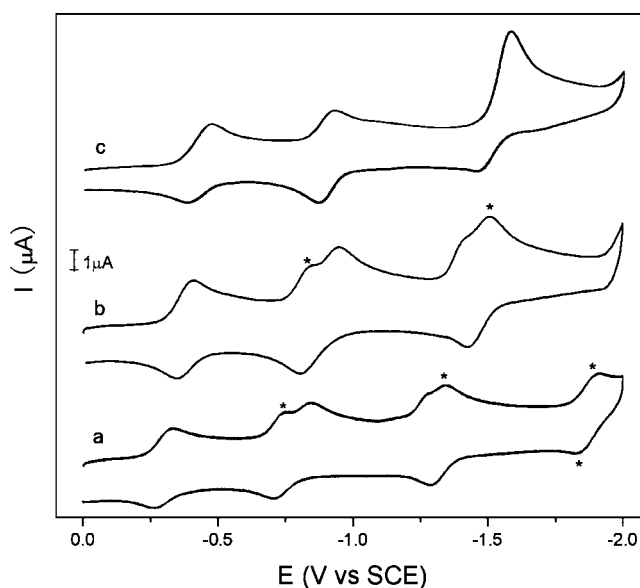


FIGURE 1. Cyclic voltammograms of compounds (a) **1**, (b) **2**, and (c) **3** in DMF containing 0.1 M TBAP at a scan rate of 100 mV/s. Only the first scan is shown for each compound. Peaks marked with asterisks show the redox process of C₆₀ in (a) and C₆₁HPh in (b).

(4) (a) Knight, B.; Martín, N.; Ohno, T.; Ortí, E.; Rovira, C.; Veciana, J.; Vidal-Gancedo, J.; Viruela, P.; Viruela, R.; Wudl, F. *J. Am. Chem. Soc.* **1997**, *119*, 9871–9882. (b) Kessinger, R.; Crassous, J.; Herrmann, A.; Rüttimann, M.; Echegoyen, L.; Diederich, F. *Angew. Chem., Int. Ed.* **1998**, *37*, 1919–1922. (c) Boudon, C.; Gisselbrecht, J.-P.; Gross, M.; Herrmann, A.; Rüttimann, M.; Crassous, J.; Cardullo, F.; Echegoyen, L.; Diederich, F. *J. Am. Chem. Soc.* **1998**, *120*, 7860–7868. (d) Crassous, J.; Rivera, J.; Fender, N. S.; Shu, L.; Echegoyen, L.; Thilgen, C.; Herrmann, A.; Diederich, F. *Angew. Chem., Int. Ed.* **1999**, *38*, 1613–1617. (e) Moonen, N. N. P.; Thilgen, C.; Echegoyen, L.; Diederich, F. *Chem. Commun.* **2000**, 335–336. (f) Beulen, M. W. J.; Rivera, J. A.; Herranz, M. A.; Illescas, B.; Martín, N.; Echegoyen, L. *J. Org. Chem.* **2001**, *66*, 4393–4398. (g) Herranz, M. A.; Beulen, M. W. J.; Rivera, J. A.; Echegoyen, L.; Díaz, M. C.; Illescas, B.; Martín, N. *J. Mater. Chem.* **2002**, *12*, 2048–2053. (h) Herranz, M. A.; Cox, C. T., Jr.; Echegoyen, L. *J. Org. Chem.* **2003**, *68*, 5009–5012.

(5) (a) Martín, N.; Altable, M.; Filippone, S.; Martín-Domenech, A.; Echegoyen, L.; Cardona, C. M. *Angew. Chem., Int. Ed.* **2006**, *45*, 110–114. (b) Lukoyanova, O.; Cardona, C. M.; Altable, M.; Filippone, S.; Domenech, A. M.; Martín, N.; Echegoyen, L. *Angew. Chem., Int. Ed.* **2006**, *45*, 7430–7433. (c) Filippone, S.; Barroso, M. I.; Martín-Domenech, A.; Osuna, S.; Solà, M.; Martín, N. *Chem.–Eur. J.* **2008**, *14*, 5198–5206.

(6) (a) Martín, N.; Altable, M.; Filippone, S.; Martín-Domenech, A.; Martínez-Álvarez, R.; Suarez, M.; Plonska-Brzezinska, M. E.; Lukoyanova, O.; Echegoyen, L. *J. Org. Chem.* **2007**, *72*, 3840–3846. (b) Delgado, J. L.; Oswald, F.; Cardinali, F.; Langa, F.; Martín, N. *J. Org. Chem.* **2008**, *73*, 3184–3188.

(7) (a) Taylor, R.; Kennard, O. *J. Am. Chem. Soc.* **1982**, *104*, 5063–5070. (b) Desiraju, G. R. *Acc. Chem. Res.* **1991**, *24*, 290–296. (c) Desiraju, G. R. *Acc. Chem. Res.* **1996**, *29*, 441–449. (d) Steiner, T. *Crystallogr. Rev.* **1996**, *6*, 1–51. (e) Houk, K. N.; Menzer, S.; Newton, S. P.; Raymo, F. M.; Stoddart, J. F.; Williams, D. J. *J. Am. Chem. Soc.* **1999**, *121*, 1479–1487.

(8) (a) Sutor, D. J. *J. Chem. Soc.* **1963**, 1105–1110. (b) Donohue, J. In *Structural Chemistry and Molecular Biology*; Rich, A., Davidson, N., Eds.; W.H. Freeman: San Francisco, CA, 1968; pp 459–463.

(9) (a) Ornstein, R. L.; Zheng, Y. J. *J. Biomol. Struct. Dyn.* **1997**, *14*, 657–665. (b) Takahara, P. M.; Frederick, C. A.; Lippard, S. J. *J. Am. Chem. Soc.* **1996**, *118*, 12309–12321. (c) Ghosh, A.; Bansal, M. *J. Mol. Biol.* **1999**, *294*, 1149–1158. (d) Loganathan, D.; Aich, U. *Glycobiology* **2006**, *16*, 343–348.

(10) (a) Bryantsev, V. S.; Hay, B. P. *J. Am. Chem. Soc.* **2005**, *127*, 8282–8283. (b) Su, Z.; Wen, Q.; Xu, Y. *J. Am. Chem. Soc.* **2006**, *128*, 6755–6760.

(11) (a) Yang, Y.; Zhang, W.; Pei, S.; Shao, J.; Huang, W.; Gao, X. *J. Mol. Struct. (THEOCHEM)* **2005**, *732*, 33–37. (b) Senthilkumar, L.; Ghanty, T. K.; Ghosh, S. K.; Kollandaivel, P. *J. Phys. Chem. A* **2006**, *110*, 12623–12628. (c) Li, Q.; An, X.; Luan, F.; Li, W.; Gong, B.; Cheng, J. *J. Phys. Chem. A* **2008**, *112*, 3985–3990.

(12) (a) Seiler, P.; Isaacs, L.; Diederich, F. *Helv. Chim. Acta* **1996**, *79*, 1047–1058. (b) Nierengarten, J.-F.; Garmlich, V.; Cardullo, F.; Diederich, F. *Angew. Chem., Int. Ed. Engl.* **1996**, *35*, 2101–2103. (c) Écija, D.; Otero, R.; Sánchez, L.; Gallego, J. M.; Wang, Y.; Alcamí, M.; Martín, F.; Martín, N.; Miranda, R. *Angew. Chem., Int. Ed.* **2007**, *46*, 7874–7877.

(13) (a) Zheng, M.; Li, F.-F.; Ni, L.; Yang, W.-W.; Gao, X. *J. Org. Chem.* **2008**, *73*, 3159–3168. (b) Li, F.-F.; Gao, X. Submitted. (c) Li, F.-B.; Liu, T.-X.; Wang, G.-W. *J. Org. Chem.* **2008**, *73*, 6417–6420.

(14) Dubois, D.; Moninot, G.; Kutner, W.; Jones, M. T.; Kadish, K. M. *J. Phys. Chem.* **1992**, *96*, 7137–7145.

the first reduction with $E_{1/2}$ at -0.30 , -0.38 , and -0.43 V versus the saturated calomel electrode (SCE) for **1**, **2**, and **3**, respectively, indicating that the monoanions of **1**, **2**, and **3** are stable on the cyclic voltammetric time scale. The observed $E_{1/2}$ values are all negatively shifted with respect to the value of C_{60} (-0.26 V versus SCE),¹⁴ while the values for **2** and **3** are negatively shifted further compared with that for **1**, consistent with previous results which show that the reduction potentials of organofullerenes are shifted cathodically as more addends are put on the sphere of C_{60} .¹⁵

However, the dianions of fullereroxazoles **1** and **2** are unstable on the cyclic voltammetric time scale, as evidenced by the appearance of an extra reduction peak during the first scan. The reduction peaks marked with asterisks at -0.75 and -0.85 V in Figure 1a and b correspond to the reduction peaks of C_{60} ¹⁴ and C_{61} HPh,¹⁶ respectively, indicating the loss of the cyclic phenylimidate group from the two compounds when **1** and **2** are reduced to the dianions. In contrast, the second reduction wave of compound **3** is clean, where a reversible one-electron redox process with $E_{1/2}$ at -0.88 V versus SCE is observed, indicating that the dianion of **3** is stable over the time frame of the electrochemical experiment.

The trianions of **1** and **2** are also unstable, as shown by the appearance of a couple of reduction peaks in each case. The reduction peaks marked with asterisks at -1.34 and -1.50 V in Figure 1a and b correspond to the third reduction peaks of C_{60} ¹⁴ and C_{61} HPh,¹⁶ indicating the formation of C_{60} and C_{61} HPh. In addition, a reversible fourth reduction wave is shown with $E_{1/2}$ at -1.86 V in the cyclic voltammogram of **1**; however, the value of the $E_{1/2}$ is the same as that for C_{60} ,¹⁴ suggesting that compound **1** decomposes to C_{60} completely upon the fourth reduction. Different from **1** and **2**, compound **3** shows only one reduction peak for the third reduction, suggesting that the trianion of **3** is still stable over the time frame of cyclic voltammetry. The cathodic peak current, however, is much larger than that for the first two reductions, probably due to an electrocatalytic reduction process mediated by the trianion of **3**. The cyclic voltammetry results clearly demonstrate that compound **3** has much more electrochemical stability than **1** and **2** under electrochemically reductive conditions, as **1** and **2** undergo the retro-cycloaddition of cyclic phenylimidate upon their reduction to dianions.

The stability of the mono- and dianionic fullereroxazoles **1–3** was evaluated further by controlled potential electrolysis (CPE), which was performed at a potential of ca. 100–200 mV more cathodic than those of the respective E_{pc} values. The resulting anionic solution was analyzed with visible and near-IR spectroscopy. The anionic solution was then oxidized back to neutral electrochemically at 0 V versus SCE, and the recovered products were analyzed by HPLC.

Visible and near-IR spectroscopy is an important method for characterization of anionic fullerene species. Anionic fullerene species have displayed characteristic absorptions in the region.¹⁷ Figure 2 shows the visible and near-IR spectra of the monoanions of **1**, **2**, and **3**. The monoanion of **1** displays broad absorption centered at 971 nm, which is blue-shifted with respect to that of monoanionic C_{60} ,^{17a–c} as previously observed for the monoanions of other C_{60} derivatives.^{17d–g} The spike at 1072

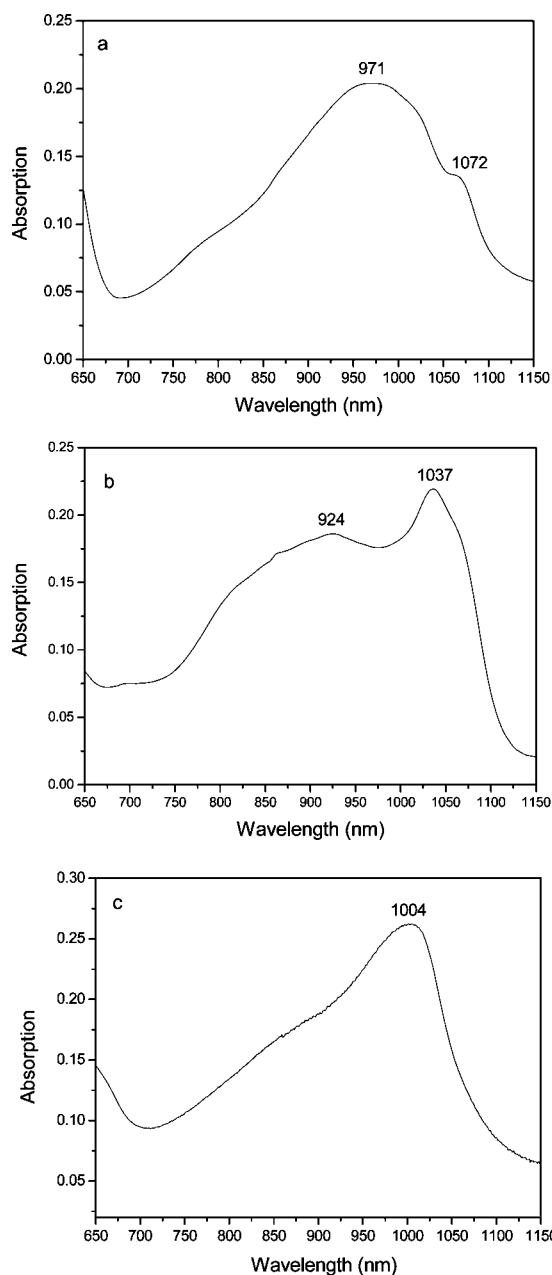


FIGURE 2. Visible and near-IR spectra of singly reduced species of (a) **1**, (b) **2**, and (c) **3** in DMF containing 0.1 M TBAP.

nm in the spectrum is due to traces of C_{60} monoanion generated from the decomposition of dianionic **1**, which is produced by slight over-reduction of monoanionic **1** (which in turn is caused during electrolysis by a considerable potential drop along the large working electrode, as described previously¹⁸). Monoanionic **2** exhibits two major absorption bands centered at 1037

(17) (a) Lawson, D. R.; Feldheim, D. L.; Foss, C. A.; Dorhout, P. K.; Elliott, C. M.; Martin, C. R.; Parkinson, B. *J. Electrochem. Soc.* **1992**, *139*, L68–L71. (b) Khaled, M. M.; Carlin, R. T.; Trulove, P. C.; Eaton, G. R.; Eaton, S. S. *J. Am. Chem. Soc.* **1994**, *116*, 3465–3474. (c) Reed, C. A.; Bolskar, R. D. *Chem. Rev.* **2000**, *100*, 1075–1120. (d) Kadish, K. M.; Gao, X.; Van Caemelbecke, E.; Hirasaka, T.; Suenobu, T.; Fukuzumi, S. *J. Phys. Chem. A* **1998**, *102*, 3898–3906. (e) Kadish, K. M.; Gao, X.; Van Caemelbecke, E.; Suenobu, T.; Fukuzumi, S. *J. Phys. Chem. A* **2000**, *104*, 3878–3883. (f) Kadish, K. M.; Gao, X.; Caemelbecke, E. V.; Suenobu, T.; Fukuzumi, S. *J. Am. Chem. Soc.* **2000**, *122*, 563–570. (g) Zheng, M.; Li, F.; Shi, Z.; Gao, X.; Kadish, K. M. *J. Org. Chem.* **2007**, *72*, 2538–2542.

(18) Rapta, P.; Bartl, A.; Gromov, A.; Stasko, A.; Dunsch, L. *ChemPhysChem* **2002**, *3*, 351–356.

(15) Echegoyen, L.; Echegoyen, L. E. *Acc. Chem. Res.* **1998**, *31*, 593–601.

(16) The E_{pc} for C_{61} HPh in DMF containing 0.1 M TBAP at a scan rate of 100 mV/s is -0.41 , -0.86 , and -1.50 V versus SCE. See the Supporting Information for the cyclic voltammogram.

and 924 nm, where the band at 1037 nm is similar to that of the monoanionic $C_{61}\text{HPh}$ (1030 nm),^{17e,g} indicating that the band at 1037 nm is related to the benzal group. The band at 924 nm is very broad, similar to that of monoanionic **1**, and likely is related to the heterocyclic phenylimidate ring in the compound. The monoanion of **3** exhibits a strong and broad absorption band centered at 1004 nm, which is red-shifted compared to the bands of the monoanions of 1,4-(PhCH₂)₂C₆₀ (989 nm)^{17e} and **1**. Notably, in contrast to the relatively sharp absorption bands for anions of alkyl-functionalized C₆₀ derivatives, the absorption peaks for monoanions of **1**, **2**, and **3** are rather broad and are probably due to the heterocyclic ring in the compound, suggesting that different types of addends affect the spectroscopic features of reduced organofullerenes differently.

Results from the experiment using the visible and near-IR spectra indicate that all of the monoanions of **1**, **2**, and **3** are stable. This observation is consistent with that made in previous literature results.⁴ The generated monoanionic species for each compound were oxidized electrochemically back to neutral and were analyzed by HPLC (see the Supporting Information), confirming that the monoanions of **1**, **2**, and **3** are stable over the time frame of electrolysis and spectral measurement.

Fulleroroxazoles **1**, **2**, and **3** were further reduced to dianions with CPE. Figure 3 shows the visible and near-IR spectra of the resulting anionic species for **1**, **2**, and **3**. The anionic **1** solution displays absorption bands at 947 and 830 nm, which is typical for the C₆₀ dianion, suggesting that the dianion of **1** undergoes a retro-cycloaddition reaction and decomposes to the parent C₆₀. The small spike at 1072 nm is due to traces of C₆₀ monoanion and is in agreement with that observed in the formation of C₆₀. Dianionic **2** exhibits the spectral feature of C₆₁HPh²⁻ by showing an absorption band at 910 nm,^{17e,g} indicating that the dianion of **2** is not stable either and undergoes a retro-cycloaddition reaction. An absorption band at 1033 nm is ascribed to C₆₁HPh⁻,^{17e,g} consistent with the occurrence of retro-cycloaddition reaction. However, the dianion of **3** shows no feature of the dianionic 1,4-(PhCH₂)C₆₀ (989 nm)^{17e} in the visible and near-IR spectrum; instead, it shows a strong absorption band at 888 nm, which is blue-shifted with respect to that of monoanion (1004 nm), consistent with the relationship for the absorption bands previously observed between dianions and monoanions,^{17d–g} suggesting that the dianion of **3** is electrochemically stable. The spike at 1004 nm is due to traces of monoanionic **3**, which is probably generated by slight oxidation during transfer of the solution prior to measurement.

In order to confirm the electrochemical stability of dianionic **1–3**, the reduced species were oxidized electrochemically back to neutral and analyzed by HPLC (see the Supporting Information), where C₆₀ and C₆₁HPh are predominant in HPLC traces from the recovered mixtures of dianionic **1** and **2**, confirming

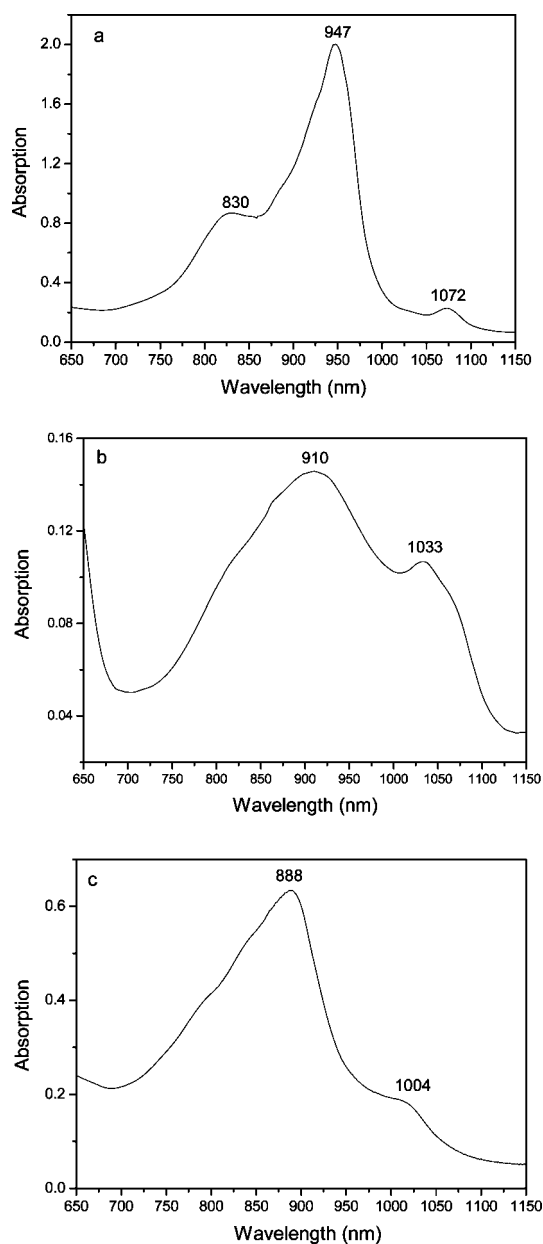


FIGURE 3. Visible and near-IR spectra for the anionic solution of (a) **1**, (b) **2**, and (c) **3** in DMF containing 0.1 M TBAP after the second reduction.

that the dianions of **1** and **2** are unstable and undergo retro-cycloaddition reactions. However, only one major fraction peak corresponding to **3** is shown in the HPLC trace of the recovered product from dianionic **3**, indicating that the dianion of **3** is stable and does not undergo retro-cycloaddition reaction.

The results show the retro-addition reactions involve only the dianionic species but not the monoanionic ones, consistent with the findings of previous work,⁴ thereby suggesting that the retro-addition reaction is a charge-induced process. Computational calculations on the NBO charge distribution based on optimized dianionic structures of **1**, **2**, and **3** were performed at B3LYP/6-31G theoretical level, using a Gaussian 03 program package.¹⁹ Figure 4 shows the NBO charge densities of the atoms that are involved in the retro-cycloaddition reactions. There is no significant difference of charge densities on these atoms among the three compounds. In fact, the corresponding atoms in **3** have the largest charge densities among the three

(19) Frisch, M. J.; Trucks, G. W.; Schlegel, H. B.; Scuseria, G. E.; Robb, M. A.; Cheeseman, J. R.; Montgomery, J. A., Jr.; Vreven, T.; Kudin, K. N.; Burant, J. C.; Millam, J. M.; Iyengar, S. S.; Tomasi, J.; Barone, V.; Mennucci, B.; Cossi, M.; Scalmani, G.; Rega, N.; Petersson, G. A.; Nakatsuji, H.; Hada, M.; Ehara, M.; Toyota, K.; Fukuda, R.; Hasegawa, J.; Ishida, M.; Nakajima, T.; Honda, Y.; Kitao, O.; Nakai, H.; Klene, M.; Li, X.; Knox, J. E.; Hratchian, H. P.; Cross, J. B.; Bakken, V.; Adamo, C.; Jaramillo, J.; Gomperts, R.; Stratmann, R. E.; Yazyev, O.; Austin, A. J.; Cammi, R.; Pomelli, C.; Ochterski, J. W.; Ayala, P. Y.; Morokuma, K.; Voth, G. A.; Salvador, P.; Dannenberg, J. J.; Zakrzewski, V. G.; Dapprich, S.; Daniels, A. D.; Strain, M. C.; Farkas, O.; Malick, D. K.; Rabuck, A. D.; Raghavachari, K.; Foresman, J. B.; Ortiz, J. V.; Cui, Q.; Baboul, A. G.; Clifford, S.; Cioslowski, J.; Stefanov, B. B.; Liu, G.; Liashenko, A.; Piskorz, P.; Komaromi, I.; Martin, R. L.; Fox, D. J.; Keith, T.; Al-Laham, M. A.; Peng, C. Y.; Nanayakkara, A.; Challacombe, M.; Gill, P. M. W.; Johnson, B.; Chen, W.; Wong, M. W.; Gonzalez, C.; Pople, J. A. *Gaussian 03*, revision D.01; Gaussian, Inc.: Wallingford, CT, 2004.

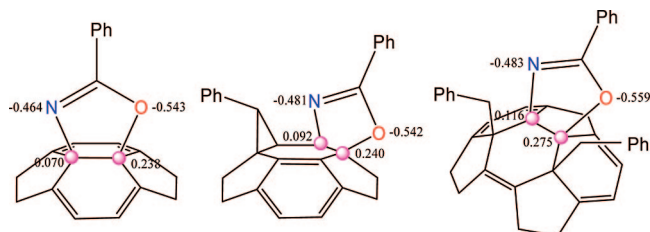


FIGURE 4. NBO charge densities on the atoms involved in the retro-cycloaddition reactions of dianions of **1**, **2**, and **3**.

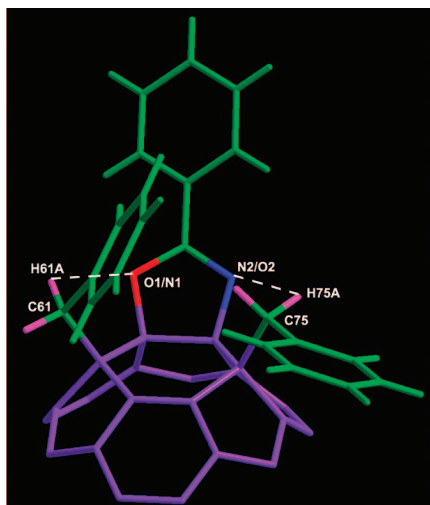


FIGURE 5. Expanded view of the crystal structure of compound **3**, with H61A...O1/N1 and H75A...N2/O2 distances shown as dashed lines.

compounds, suggesting that **3** should be the most electrochemically unstable compound, where charge density is the only factor determining stability. This scenario contrasts with the experimental results, thereby implying the existence of other factors which govern the electrochemical stability of the compounds.

Interactions among the addends in organofullerenes may account for the different behavior of the compounds. C–H...X (X = O, N) hydrogen bonding has been shown to play important roles in formation and stabilization of complexes, although it is a weak interaction.^{7,8a,10} The presence of both nitrogen and oxygen atoms, as well as that of the C–H bonds in **3**, makes it possible that such bonding can occur between the addends of the compound. Close examination on the X-ray single-crystal structure of compound **3**^{13a} (as shown in Figure 5) indicates the possible existence of intramolecular hydrogen bonding between cyclic phenylimidate and the two benzylys positioned in vicinity, with H61A...O1/N1 and H75A...N2/O2 being only 2.29 and 2.39 Å, respectively, which are much shorter than the sum of van der Waals radii of H with O or N (H = 1.20, O = 1.40, N = 1.50 Å).²⁰ However, the bond angles for C61–H61A...O1/N1 and C75–H75A...N2/O2 are only 104.0 and 93.4°, respectively, with these values being close to the geometric criteria for C–H...X hydrogen bonding, though still within the generally accepted bond angles.^{7a}

The presence of C–H...X hydrogen bonding in **3** is further supported by NBO analysis,¹¹ which has been shown to be a

reliable method in the evaluation of hydrogen bonds since it can derive information on the changes of charge densities in proton donors and acceptors, the population of lone pairs and antibonding orbital ($\sigma^*(\text{C}-\text{H})$) involved in the hydrogen bond, as well as the stabilization energy ($E^{(2)}$) associated with $i-j$ delocalization given by $E^{(2)} = q_i(F_{ij})^2/(\epsilon_j - \epsilon_i)$, where q_i is the donor orbital occupancy, ϵ_j and ϵ_i are orbital energies, and F_{ij} is the off diagonal NBO Fock matrix element. Results from an NBO analysis of **3** show occupation numbers of lone pairs of N and O in the proton acceptors are 1.8921 and 1.9643, respectively, and occupation numbers of antibonding orbital $\sigma^*(\text{C}-\text{H})$ are 0.0114 and 0.0099, respectively, for C–H...N and C–H...O hydrogen bonds. The second-order perturbation energy values ($E^{(2)}$) due to $n(\text{N}) \rightarrow \sigma^*(\text{C}-\text{H})$ and $n(\text{O}) \rightarrow \sigma^*(\text{C}-\text{H})$ orbital interactions are 0.69 and 0.45 kcal/mol, respectively, which contribute significantly to the stabilization of C–H...N and C–H...O hydrogen bonds in the compound. In addition, a more negative charge is shown on the N and O atoms in **3** (N = -0.485, O = -0.545) than that in **1** (N = -0.469, O = -0.528), while more positive charges are exhibited on the C–H protons in **3** (0.278, 0.280) compared to those in 1,4-(PhCH₂)₂C₆₀²¹ (H = 0.264, 0.259), which is consistent with the formation of intramolecular C–H...X hydrogen bond in **3**.

The formation of such hydrogen bonding is also supported by the ¹H NMR spectrum, where one set of methylene protons from each benzyl bonded to C₆₀ appear at 5.03 and 4.94 ppm,^{13a} which are significantly downfield-shifted compared with that of the other set of methylene protons (4.51 and 4.49 ppm) and 1,4-(PhCH₂)₂C₆₀ (3.73 ppm),^{17e} consistent with the proposed H-bonds. In addition, the greatly downfield resonances for methylene protons indicate that the protons are very acidic, which also facilitates the formation of intramolecular C–H...N and C–H...O hydrogen bonds since increasing the acidity of the hydrogen donor leads to shorter and stronger C–H...N/O bonds.^{7b,10b}

As for compound **1**, it is not surprising that no such intramolecular hydrogen bonding is formed since no proton donor is available. While compound **2** has a methyne proton available next to the nitrogen atom (as the X-ray single-crystal shows), however, the H...N distance is 2.68 Å,^{13b} which is much greater than that in **3** and is almost the same as the sum of van der Waals radii of H with N,²⁰ indicating that no C–H...N hydrogen bond is formed. In addition, ¹H NMR of **2** shows that the methyne proton has a resonance at 5.06 ppm,^{13b} which is upfield-shifted with respect to that of C₆₁HPh (5.38 ppm),^{17g} suggesting that the C–H is actually more shielded with increasing electron density, implying that the C–H does not act as a proton donor and that there is no interaction between the benzal C–H and the neighboring nitrogen atom in **2**. The heterocyclic ring in **1** and **2** is therefore unstable due to the absence of C–H...X hydrogen bonding, while it is stabilized in **3** due to the presence of the weakly intramolecular C–H...X hydrogen bonds formed among the addends, so that no decomposition occurs under two-electron-transfer reductive electrolysis.

Conclusions

Different electrochemical behavior is observed for the structurally related fullerooxazoles **1–3**, where the heterocyclic ring in **1** and **2** is removed under two-electron-transfer reductive conditions, while under similar conditions, it is retained in **3**. X-ray crystal structure of **3** indicates the presence of intramolecular C–H...N/O hydrogen bonding,

(20) (a) Cady, H. H. *Acta Crystallogr.* **1967**, *23*, 601–609. (b) Choi, C. S.; Boutin, H. P. *Acta Crystallogr.* **1970**, *B26*, 1235–1240. (c) Choi, C. S.; Abel, J. E. *Acta Crystallogr.* **1972**, *B28*, 193–201.

(21) Subramanian, R.; Kadish, K. M.; Vijayashree, M. N.; Gao, X.; Jones, M. T.; Miller, D. M.; Krause, K.; Suenobu, T.; Fukuzumi, S. *J. Phys. Chem.* **1996**, *100*, 16327–16335.

an observation which is rationalized with the NBO analysis. The results suggest that the intramolecular C–H···N/O hydrogen bonding is the key factor for the electrochemical stability of the dianion of **3**. To the best of our knowledge, this is the first time that weak intramolecular hydrogen bonding has been shown to make a significant contribution to the electrochemical stability of organofullerenes. The findings may shed light on the design and synthesis of functionalized fullerenes with high stabilities.

Acknowledgment. The work was supported by Hundred Talents Program of the Chinese Academy of Sciences, NSFC

International Collaboration Grants 00550110367 and 00650-110171.

Supporting Information Available: General experimental methods, cyclic voltammogram of C₆₁HPh in DMF containing 0.1 M TBAP at a scan rate of 100 mV/s, HPLC traces of the recovered neutral substances oxidized electrochemically from monoanionic and dianionic **1**, **2**, and **3**. Optimized Cartesian coordinates of **1**, **2**, and **3** dianions and **3**, **1**, and 1,4-(PhCH₂)₂C₆₀ for NBO analysis. This material is available free of charge via the Internet at <http://pubs.acs.org>.

JO801769Q